

Assessing the effects of voluntary and involuntary eyeblinks in independent components of electroencephalogram

Suguru Kanoga ^{a,*}, Masaki Nakanishi ^b, Yasue Mitsukura ^a

^a School of Integrated Design Engineering, Keio University, Yokohama, Kanagawa, Japan

^b Swartz Center for Computational Neuroscience, Institute for Neural Computation, University of California, La Jolla, San Diego, CA, USA

ARTICLE INFO

Article history:

Received 30 July 2015

Received in revised form

28 October 2015

Accepted 5 January 2016

Communicated by: S. Hu

Available online 10 February 2016

Keywords:

Eyeblinks

Electroencephalographic signals

Artifacts

Independent component analysis

Wavelet transform

ABSTRACT

The effect of voluntary and involuntary eyeblinks in independent components (ICs) contributing to electroencephalographic (EEG) signals was assessed to create templates for eyeblink artifact rejection from EEG signals with small number of electrodes. Fourteen EEG and one vertical electrooculographic signals were recorded for twenty subjects during experiments that prompted subjects to blink voluntarily and involuntarily. Wavelet-enhanced independent component analysis with two markers was employed as a feature extraction scheme to investigate the effects of eyeblinks in ICs of EEG signals. Extracted features were separated into epochs and analyzed. This paper presents following characteristics: (i) voluntary and involuntary eyeblink features obtained from all channels present significant differences in the delta band; (ii) distorting effects have continued influence for 3.0–4.0 s (in the occipital region, 2.0 s); and (iii) eyeblink effects cease to exist after the zero-crossing four (in the occipital region, two times, regardless of the type. Several characteristics are different between voluntary and involuntary eyeblinks in EEG signals. Therefore, any templates need both types of data for eyeblink artifact rejection if the EEG signals were obtained from small number of electrodes.

© 2016 The Authors. Published by Elsevier B.V. This is an open access article under the CC BY-NC-ND license (<http://creativecommons.org/licenses/by-nc-nd/4.0/>).

1. Introduction

Kaleidoscopic functional states of the cerebral cortex affected by neuronal activities (nerve firings) can be measured using an electrical non-invasive index, in the form of an electroencephalographic (EEG) signal. The EEG signal is the useful clinical tool for the diagnosis of psychiatric disorders such as schizophrenia and epilepsy, and for studying the functional states of the brain [1,2]. In addition, EEG signals have been widely used in brain-computer interface (BCI) systems that provide communication channels to people with severe motor disabilities [3,4]. Over the past three decades, the spatio-temporal event-related neural dynamics revealed from various experimentally manipulated events and interpretation of EEG signals have been developed to integrate dynamics with practical applications.

The good conductivity of the scalp leads to contamination of recorded EEG signals with potentials generated from movement of the eyelid and/or the eyeball, which may affect on delta (0.5–4.0 Hz), theta (4.0–8.0 Hz), and alpha (8.0–13.0 Hz) bands [5,6]. Eyeblink artifacts are extremely burdensome when investigating neuronal activities using EEG signals because the EEG spectrum is superimposed with the

artifacts [7]. Furthermore, the amount of oscillating neuronal discharge (EEG potential) is generally lower than the artifact potential at each electrode [8]. The effects of eyeblinks on EEG signals depend on the orientation of the eyeball, the trajectory of the eyelid, the location of the electrode on the scalp, and the propagation path of the electric field across the head [9,10]. Although researchers are able to avoid the issue by giving an instruction that asks subjects to keep their eyes closed during the EEG measurement, any constructed system based on the research would be impractical in the real world because of the necessity of having users close their eyes while the system operates. In addition, the inhibition of eye movements or eyeblinks significantly distorts the neuronal activity [11]. Therefore, EEG signals should be recorded with the eyes open and without any constraints to allow investigation into intrinsic endogenous brain activities, even if the eyeblink artifactual contamination of the EEG signal cannot be avoided because of the structure of human body.

Regression-based approaches include the well-known ocular artifact removal method for investigating plausible neuronal activities with the eyes open [12]. In this approach, propagation factors are calculated using linear least-square regression to estimate the relationship between the recorded electrooculographic (EOG) signals and the recorded EEG signals of each channel [13]. By subtracting the eyeblink artifact coordinated by the propagation factors, regression procedures remove eyeblink artifacts from each channel at a low computational cost. However, eyeblinks vary

* Corresponding author. Tel.: +81 45 566 1718.

E-mail address: kanouga@mitsu.sd.keio.ac.jp (S. Kanoga).

their amplitudes and durations according to the movement of the eyelid [14] and whether the blink occurs under voluntary or involuntary control [8,15]. For this property, the approximation performance of linear regression depends on the distribution of eyeblink amplitude and duration in the data set [16]. Furthermore, bidirectional contamination between EEG and EOG signals has been revealed; therefore, relevant cerebral information interfered with the EOG signal would also be canceled in the EEG signal corrected using a regression-based approach [17].

Eyeblink artifacts observed in EEG signals have the following properties: (i) the influence of the artifact is attenuated with increasing distance from the eyes [18]; and (ii) the activity of the artifacts appears to propagate along the anterior-posterior axis in a symmetrical fashion [5,8]. On the basis of these properties, theoretically multivariate statistical analysis approaches such as principal component analysis and independent component analysis (ICA), which separate EEG signals into spatially and temporally distinguishable components, are useful for extracting EEG components from the scalp recordings [19,20]. In particular, ICA is a powerful tool for separating the recorded EEG signals into maximally independent activity patterns derived from cerebral or non-cerebral (artifactual) sources [21]. ICA-based approaches have shown an extraordinary ability to solve blind source separation problems using the assumption of independence among signal sources in each subject's data. These approaches have been used in a wide range of EEG signal processing procedures for the removal of eyeblink artifact components from recorded EEG signals [22] and the extraction of signals of interest to improve the overall performance [23], regardless of the distribution of blink amplitude and duration. In comparison with the regression-based approach, the ICA-based approach accurately eliminates eyeblink artifacts from EEG signals with less loss of cerebral information [24].

A smaller number of electrodes (i.e., the single-electrode case would be an extreme case) should result in better practical applications in daily life. Single-channel ICA, which is an adaptation of ICA to single-channel signals, has been proposed [25]; however, the scheme does not always satisfy its assumptions in real-world applications. Therefore, proposing an eyeblink artifact removal scheme for a single-channel EEG signal is now a major challenge within EEG signal processing [26,27]. To avoid an inconsistency in separating components of a single-channel EEG signal that has overlapping frequency components, reference data helps experimental data to converge to the values of estimated sources in the aforementioned schemes. In addition, the presence of involuntary eyeblink artifacts in the target signal leads to a distorted signal after applying the reference-based scheme, because the reference is usually based only on voluntary eyeblink data. Although several research has analyzed the pattern of eyeblink artifacts to develop eyeblink artifact removal methods for multichannel EEG signals, the effect of involuntary eyeblinks on scalp EEG signals is still missing [22,28]. This study investigates the plausible effects of voluntary and involuntary eyeblinks on scalp EEG signals using multichannel ICA. Since recent studies have suggested wavelet-enhanced ICA algorithm is suitable for separating EEG signals into cerebral and non-cerebral sources [29], this study employed this method. Investigation of eyeblink artifacts under voluntary and involuntary control lead to development of more robust and more common references or training datasets based on the representative attributes for small number of channels in EEG analysis. Therefore, the objective of this paper is to characterize the effects of voluntary and involuntary eyeblinks on independent components (ICs) contributing to EEG signals by wavelet-enhanced ICA to create templates for eyeblink artifact rejection from a recorded EEG signal with a single-electrode.

2. Materials and methods

2.1. EEG and EOG recordings

In this paper, EEG signals were recorded at 14 positions (Fp1, Fp2, F3, F4, T3, C3, Cz, C4, T4, P3, Pz, P4, O1, and O2) according to the 10–20 system. Active electrodes for EEG data were made of sintered Ag/Ag–Cl material (g.tec Medical Engineering GmbH, Austria) and their metallic tips were attached to the scalp. A vertical EOG signal was recorded from two surface Ag/Ag–Cl electrodes (Blue Sensor P, Ambu Corp., Denmark) placed at the superior and inferior orbital rims of the left eye. Reference and ground electrodes were placed at the left mastoid and Fz, respectively. The EEG and EOG data were band-pass filtered from 0.5 Hz to 60 Hz with a Butterworth filter and digitized at a sampling rate of 256 Hz using g.USBamp. The first 5 s of recorded data is discarded. All electrodes were pasted with an electrolyte, g. GAMMAgel, to reduce skin resistance.

Twenty subjects (14 males and 6 females, mean age: 22.75 ± 1.45 years, 14 right and 6 left eye dominants) participated in the experiments. No subjects had a history of sensorimotor, ophthalmologic, or auditory abnormalities. All subjects were asked to read and sign an informed consent approved by the Research Ethics Committee of Keio University prior to participating the study. None of the subjects were permitted to wear eyeglasses and all used canal-type earphones during the experiments.

2.2. Stimuli and procedure

Each subject was seated in a dim room (mean illuminance: 188.95 ± 24.50 lx) in front of a laptop PC. The distance between subject and display was roughly 60 cm and the third highest lightness-contrast was selected, while displaying a cross-fixation on the display. During the experiments, the subject's face was video recorded using a tablet PC fixed to the frame of the monitor. The experimental procedure was written in Matlab using the Psychophysics Toolbox extensions [30], as follows.

2.2.1. Exp. 1 (for voluntary eyeblink)

An audio file (Windows Background.wav, 55.0 dB), which is used as an alert sound (a beep) in the Windows 8.1 operating system was used to obtain voluntary eyeblink data. The task is simply to focus on a black cross-fixation in the center of the display and to blink with both eyes within 1 s after the sound stimulus (see Fig. 1(A)). The simple auditory stimulus was repeated for this experiment to avoid interference with other eye-related potentials: (i) the occipital positive potential (the lambda wave) that is an evoked potential based on the changed visual stimulus, which typically occurs roughly 300 ms after the onset of a blink [31]; (ii) the cerebral potential caused by the efference copy, which represents a process for anticipation of the change in the visual stimulus from the eye-movement [32]. In each of the experiments, the subject was instructed to blink naturally, in addition to the prescribed blinks, and not to blink stiffly or strongly, but instead, to simply react quickly. The datasets for each subject consist of 3 sessions. Each session includes 20 trials; the next session is started after a 60-s resting period to maintain ocular moisture. Whereas normal adults blink every 3.0 s, a sound was presented every 5.0 or 6.0 s in a randomized order. In short, subjects had to blink in a slightly unusual way. However, the presentation interval was deliberately decided (as mentioned above) because we experimentally found that the effects of eyeblink on EEG signals have continued their influence for 3.0–4.0 s.

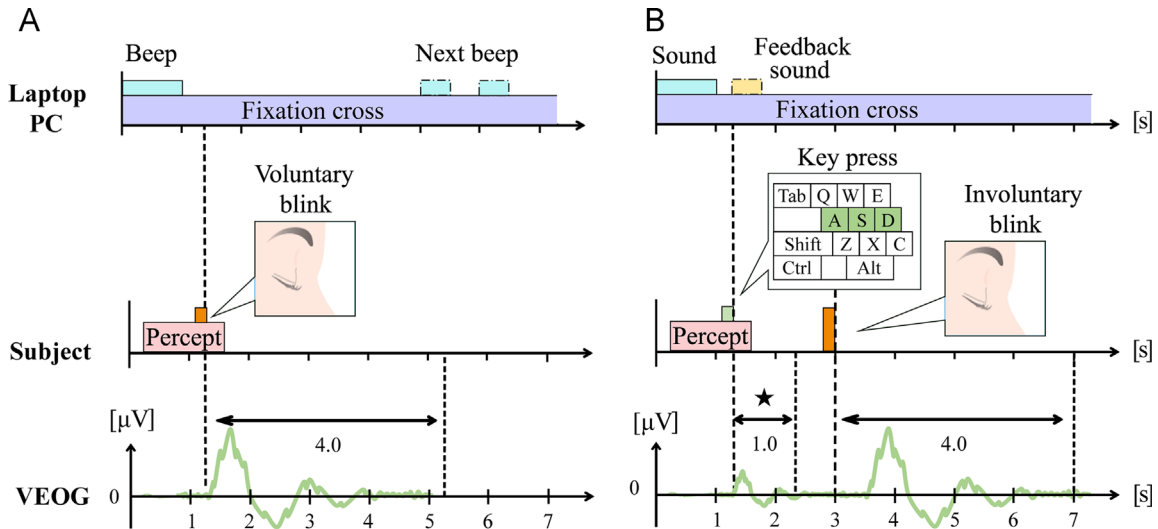


Fig. 1. (A) Diagram of a trial for voluntary eyeblink. The 4-s epoch was used for analysis. However, the entire time period was used for calculating ICA spatial filtering. (B) Diagram of a trial for involuntary eyeblink. The 4-s epoch, excluding the period indicated by the black star, was used for analysis. However, the entire time period was also used for calculating ICA spatial filtering.

2.2.2. Exp. 2 (for involuntary eyeblink)

Three sounds called "A" (440.0 Hz, 55.0 dB), "S" (554.0 Hz, 55.0 dB), and "D" (659.0 Hz, 55.0 dB) were prepared to obtain involuntary eyeblink data. One of the three sounds (in a randomized order) is presented for 1 s after 10–14 s. During the experiments, subjects put their left fingertips (the ring finger, the middle finger, and the index finger) on the "A", "S", and "D" keys of the keyboard (see Fig. 1(B)). The subject presses the key corresponding to the associated sound after the sound stimulus. Then, a feedback sound is presented to the subject in accordance with the answer. After 20 trials, the rate of correct answers is shown on the display. In each of the experiments, the subject was instructed to attempt to answer 90% of the total trials correctly and to fix their eyes at the central black cross-fixation. There were no other restrictions, meaning the subject could blink naturally (involuntarily). The datasets of each subject consist of 3 sessions.

2.3. Feature extraction scheme

In this paper, the information maximization (infomax) ICA algorithm [19] is employed as the signal separation scheme to obtain ICs and relative projection strengths. Furthermore, double thresholds based on indexes of modified multiscale sample entropy (mMSE) and kurtosis are employed to automatically classify the ICs as either neuronal or artifactual. Then, the identified artifactual ICs are carefully purified using biorthogonal wavelets to extract eyeblink features from the recorded signals. Finally, the extracted features are used to assess the effects of voluntary and involuntary eyeblink on ICs contributing to EEG signals.

2.3.1. ICA-based signal separation

ICA is the most popular scheme for separating multi-channel observed signals $\mathbf{x}(n) = [x_1(n), x_2(n), \dots, x_p(n)]^T$ into statistically independent source signals $\mathbf{s}(n) = [s_1(n), s_2(n), \dots, s_q(n)]^T$ [20,21]. The observed signals are assumed to consist of signals that are linear combinations of unknown, and statistically- q -independent source signals. In addition, we assume that the number of independent sources is equal to or lower than the number, p , of observation signals. The ICA algorithm determines the mixing

matrix \mathbf{M} that defines the weights with which each estimated source is present in the recorded EEG data.

$$\mathbf{x}(n) = \mathbf{M} \mathbf{s}(n), \quad (1)$$

where the unknown mixing matrix \mathbf{M} is a square $p \times p$ matrix. In this paper, the number of electrodes for EEG recording is 14; therefore, $p = 14$. The matrix gives the relative projection strengths of the respective ICs to each of the scalp electrodes [17]. There are several kinds of ICA algorithm for accuracy improvement for source separation. In this paper, we apply the logistic infomax ICA algorithm that has been implemented using the *runica* function in the EEGLAB Matlab toolbox [33] with its default settings. This scheme separates the original signals into the same number of ICs ($p = q = 14$).

After ICA-based signal separation, each IC is suspended as an artifactual component and identified as an artifactual or neuronal IC using specific steps (visual inspection, thresholding, and so on). Then, intrinsic (non-artifact) EEG signals and artifacts are spuriously separated using the inverse ICA linear demixing process.

2.3.2. Automatic component identification

ICA gives us the ability to investigate the plausible effects of eyeblink on recorded EEG signals based on the two assumptions described above and an assumption that propagation delays through the mixing medium (i.e., brain, scalp, and body) are negligible. Visual inspection of scalp topographies and correlation analysis of the IC that has the highest correlation with the recorded vertical EOG signal have been conducted for identifying the ocular artifacts in ICs from recorded EEG signals [34,35]. However, eyeblink artifacts are allocated to one or more ICs, meaning that the identification steps are sometimes not able to accurately select the correct components. This year, the issue was solved by combining ICA with a wavelet transform (WT) [36]. The new scheme automatically identifies artifactual components using double thresholds based on the indeces of mMSE and kurtosis.

The index of mMSE is based on the concept of sample entropy, which is an index quantifying the regularity and complexity of data. Given the p -th estimated IC $\{\hat{s}_p(n) : 1 \leq n \leq N_s\}$ by logistic infomax ICA that has N_s data points, the following vector sequence is formed:

$$\hat{S}_i^m = \{\hat{s}_p(i), \hat{s}_p(i+1), \dots, \hat{s}_p(i+m-1)\} - \hat{s}_p(0) \quad (i = 1, \dots, N_s - m + 1), \quad (2)$$

$$\hat{s}_p 0(i) = \frac{1}{m} \sum_{j=0}^{m-1} s_p(i+j), \quad (3)$$

where $\hat{s}_p 0(i)$ and m are a baseline for generalization of the vector sequence and the maximum length of epochs for matching templates, respectively. The minimum length is set to 2 (i.e., $m = 2$). Despite the fact that the actual number of data points is N (25,600 to 31,920 in the Exp.1 and 51,200 to 71,680 in the Exp. 2), the first 10 s of data (i.e., $N_s = 2560$) is used in this step.

Then, the distance between two vectors is defined as

$$d_{ij}^m = d[\hat{s}_i^m, \hat{s}_j^m] \\ = \max_{h \in (0, m-1)} |\hat{s}_p(i+h) - \hat{s}_p 0(i) - (\hat{s}_p(j+h) - \hat{s}_p 0(j))| \quad (i, j = 1, \dots, N_s - m, j \neq i), \quad (4)$$

and the degree of similarity between vectors is defined using Eq. (2).

$$D_{ij}^m = f(d_{ij}^m, r) = \frac{1}{1 + \exp[(d_{ij}^m - 0.5)/r]}, \quad (5)$$

where r is the tolerance or the slope of the Sigmoid function. In this paper, we set the value at $0.2\sigma_{\hat{s}_p}$ ($r = 0.2 \times \sigma_{\hat{s}_p}$). The input pattern assesses its belongingness to a given class using the continuous boundary, instead of the Heaviside function [37]. Furthermore, functions B and A , which are used to count m and $(m+1)$ template matches within the tolerance, are defined as

$$B_r^m(i) = \frac{1}{N_s - m - 1} \sum_{j=1, j \neq i}^{N_s - m} D_{ij}^m, \quad (6)$$

$$B_r^m = \frac{1}{N_s - m} \sum_{i=1}^{N_s - m} B_r^m(i), \quad (7)$$

$$A_r^m(i) = \frac{1}{N_s - m - 1} \sum_{j=1, j \neq i}^{N_s - m} D_{ij}^{m+1}, \quad (8)$$

$$A_r^m = \frac{1}{N_s - m} \sum_{i=1}^{N_s - m} A_r^m(i). \quad (9)$$

Finally, index of mMSE is defined by using negative natural logarithm of deviation of B_r^m from A_r^m ,

$$\text{mMSE}(m, r) = \lim_{N_s \rightarrow \infty} (\ln B_r^m - \ln A_r^m), \quad (10)$$

$$\text{mMSE}(m, r, N_s) = -\ln(A_r^m / B_r^m). \quad (11)$$

The index of mMSE with a 95% confidence interval (CI) of the mean in the Student's t -distribution is used for the threshold for detecting eyeblink artifactual ICs using the following equation:

$$\text{Threshold}_1 = m_{\text{mMSE}} - \frac{\sigma_{\text{mMSE}}}{\sqrt{N_s}} \times t_{N_f}, \quad (12)$$

where m_{mMSE} , σ_{mMSE} , and t_{N_f} are the mean of mMSE, the standard deviation of mMSE, and the index in the t -distribution with 13 degrees of freedom ($N_f = p - 1$). An artifactual IC is expected to have a value of mMSE that is less than that of a neuronal IC.

One index of kurtosis is the fourth-order cumulant, which is used to characterize the location and variability of data and is a measure of whether the variables are peaked or flat relative to a Gaussian distribution.

$$\text{kurtosis}_p = m_{p_4} - 3m_{p_2}^2, \quad (13)$$

$$m_{p_c} = E\{(\hat{s}_p - m_{p_1})^c\}, \quad (14)$$

where m_{p_c} , m_{p_1} and E are the c -th order central moment of the variable, its mean, and the expectation function of the p -th IC. In this paper, we calculated the kurtosis using the *kurtosis* function of

Matlab for each IC. Eyeblink activities can be effectively detected by combining this index with mMSE because kurtosis is positive for peaked spasmodic activities [38]. Therefore, the index of kurtosis with a 95% CI for the mean is used for the threshold to detect eyeblink artifactual ICs based on the following equation:

$$\text{Threshold}_2 = m_{\text{kurtosis}} + \frac{\sigma_{\text{kurtosis}}}{\sqrt{N_s}} \times t_{N_f}, \quad (15)$$

where m_{kurtosis} and σ_{kurtosis} are the mean and the standard deviation of kurtosis.

All of the ICs with mMSE and kurtosis values that are outside the double thresholds are identified as eyeblink artifactual ICs.

2.3.3. Wavelet-enhanced ICA

There may be cases in which a contradiction occurs between the ICA assumption and the neural patterns of activation because neural networks are often overlapping (not independent). ICs presenting artifactual activities obtained from the stimulus-presenting analysis, especially in the event-related potential analysis, might have distinctive interfering neuronal activities in the components. Discarding all components will lead to loss of neuronal data in the ICA procedure. The wavelet-enhanced ICA algorithm uses wavelet thresholding of ICs as an intermediate step. This step allows recovery of substantial parts of the neural signal with artifacts and extraction of eyeblink artifactual components from identified artifactual ICs, all of which is done automatically [29]. All identified artifactual ICs are passed to the following thresholding procedure.

- 1) The identified artifactual ICs \hat{s}_p are transformed into components of disjointed spectra (a matrix) instead of signals (vectors) via the discrete wavelet transform (DWT).

$$W(a, b) = \frac{1}{\sqrt{a}} \int \hat{s}_p(n) \psi_{a, b}(n) dn, \quad (16)$$

$$\psi_{a,b} = \psi\left(\frac{n-b}{a}\right), \quad (17)$$

where $W(a, b)$ and $\psi_{a,b}$ denote the wavelet representation of $\hat{s}_p(n)$ and the mother wavelet, respectively, with a and b defining the time-scale and location. Usually, the time-scale a and location b are defined as $a = 2^l$ and $b = k2^l$ where l and k denote the level of decompositions and temporal localization at the level, respectively. DWT must be applied to select the mother wavelet and level of the decompositions. In this paper, the mother wavelet and level of decompositions were set to Daubechies-4 and five, respectively, implemented using *db4* in the *liftwave* function of Matlab.

- 2) If the wavelet coefficient $W(a, b)$ of each level l is lower than the wavelet threshold, the coefficient will be set to $W'(l, k) = 0$. The threshold value is defined as

$$\text{Threshold}_3 = \sigma \sqrt{2 \ln N}, \quad (18)$$

where

$$\sigma^2 = \frac{\text{median}(|W(l, k)|)}{0.6745}, \quad (19)$$

estimates the magnitude of the neuronal wideband signal with a constant value of 0.6745, related to Gaussian noise [29], and N is the length of the data.

- 3) Enhanced eyeblink artifactual ICs \hat{s}'_p are reconstructed from the thresholded wavelet coefficients $W'(l, k)$ via inverse DWT.
- 4) Fourteen-channel eyeblink artifacts in recorded EEG signals are reconstructed using the inverse ICA linear demixing process.

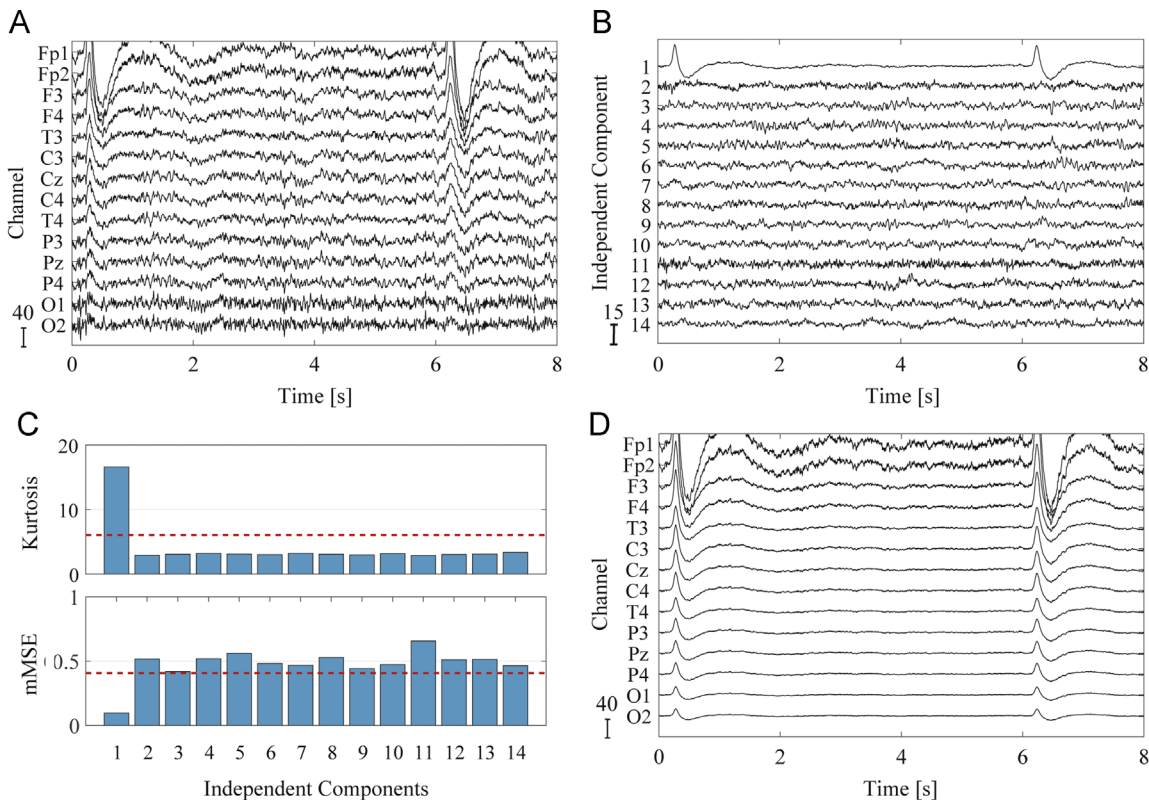


Fig. 2. Separation of EEG data including voluntary eyeblinks by wavelet-enhanced ICA. (A) An 8-s EEG signals. (B) ICs of the 14-channel signals. (C) Calculated kurtosis, mMSE (blue bars), and thresholds (red dashed lines) with 95% CI for the mean for both markers in regard to 14 ICs. The first IC was classified as an artifactual component using the markers. (D) Extracted voluntary eyeblink features of 14-channel signals. (For interpretation of the references to color in this figure legend, the reader is referred to the web version of this article.)

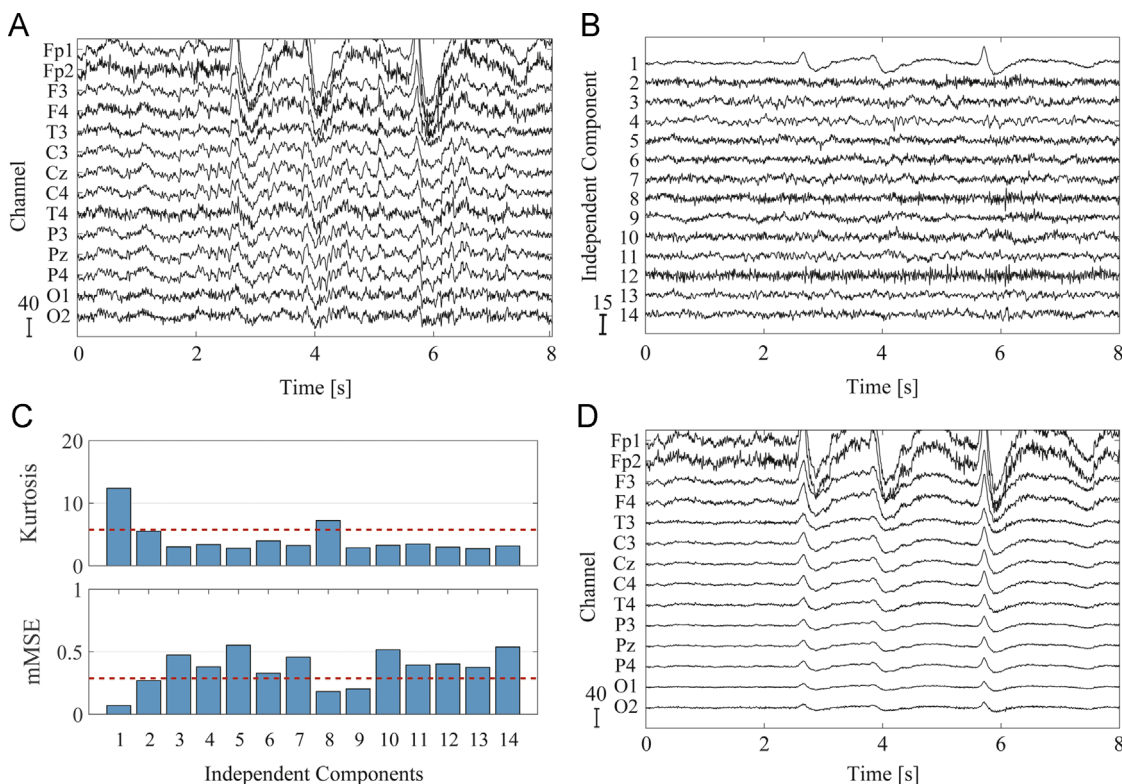


Fig. 3. Separation of EEG data including involuntary eyeblinks by wavelet-enhanced ICA. (A) An 8-s EEG signals. (B) ICs of the 14-channel signals. (C) Calculated kurtosis, mMSE (blue bars), and thresholds (red dashed lines) with 95% CI for the mean for both markers for the 14 ICs. The first and eighth ICs were classified as artifactual components based on the markers. (D) Extracted involuntary eyeblink features of 14-channel signals. (For interpretation of the references to color in this figure legend, the reader is referred to the web version of this article.)

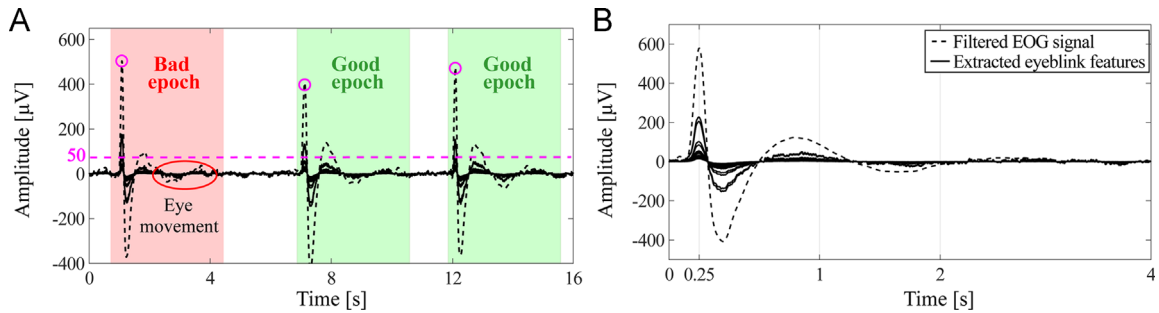


Fig. 4. (A) Peak detection using a hard threshold (pink dashed line) and epoch selection by visual inspection. Right two epochs are selected as exemplary signals that have only blink effects in the epochs. (B) A filtered vertical EOG signal (black dashed line) and extracted eyeblink features in EEG signals (black solid lines) that first positive peaks of amplitude are aligned at time 0.25 s (64th sampling point). (For interpretation of the references to color in this figure legend, the reader is referred to the web version of this article.)

2.4. Extracted eyeblink features

Figs. 2(A) and 3(A) show an 8-s EEG signals that includes voluntary and involuntary eyeblinks from subject data measured at 14 scalp positions. 2 or 3 eyeblink artifacts appear on all channels; frontal positions (e.g., Fp1, Fp2, F3, and F4) show large eyeblink effects in the data. The ICA algorithm separated the contributions of neuronal and artifactual components into 14 ICs [Figs. 2(B) and 3(B)]. In this paper, each IC was classified as either artifactual or neuronal on the basis of double thresholds and indices of mMSE and kurtosis [Figs. 2(C) and 3(C)] and blink-origin components were extracted from the identified artifactual ICs via a wavelet threshold. The extracted eyeblink features [Figs. 2(D) and 3(D)] are used to assess the effects of voluntary and involuntary eyeblink on ICs contributing to EEG signals.

2.5. Analysis of epochs

As shown in the previous section, we obtained consecutive 14-channel eyeblink features for 20 subjects.

Here, we also have consecutive vertical EOG signals. All channel features are separated into 4-s epochs to obtain time-locked data. The method for separating the epoch is determined from the vertical EOG signal. First, each recorded EOG signal passes through a Butterworth low pass filter whose cutoff frequency is 8.0 Hz, so as to reduce the cerebral activities in the EOG signal [18]. Second, the first positive peaks of blinks in the filtered EOG signal are detected using a hard threshold. The threshold value was set to 50 μ V (common to all EOG signals). A value exceeding the threshold is compared to the adjacent 50 sampling points (roughly ± 0.20 s). In this paper, if the detected value is the highest in the range, the value is further classified as to whether it is an actual peak or not by visual inspection; then, it is identified as the first positive peak of the blink. Third, 14-channel eyeblink features and a vertical EOG signal are separated into 4-s epochs based on the point of maximum amplitude in the EOG data. The point is located at the 64th sampling point (i.e., 0.25 s). An epoch, as defined above, is shown in Fig. 4.

In the Exp. 2, there is no restriction on the times and duration of blinks. Selecting an exemplary signal that has only a blink effect in its own epoch is needed to compare the voluntary eyeblink characteristics. However, it is difficult to control conscious eyelid motion, although each subject was instructed to blink only after cue presentation in the Exp. 1. Subject's eyelids sometimes quivered convulsively during motion execution; there were also instances in which two (or more) blinks were reflexively induced. Therefore, the identified epochs were carefully selected as a dataset to avoid contaminating other motions, e.g., eye movement and body motion based on video recordings and visual inspections [see Fig. 4(A)]. The number of voluntary and involuntary eyeblink

epochs obtained from each subject and the total number of the epochs are presented in Table 1. The amounts of data are uneven, however, the numerical range of differences between voluntary and involuntary for each subject lies within ± 10 , except for three subjects (Sub. 01, Sub. 09, and Sub. 20).

The eyeblink artifacts contributing to EEG signals are characterized with their respective epochs in the frequency-domain, time-frequency-domain, and time-domain. In this paper, we assessed the following three phenomena: (i) propagation effects across the head (in a symmetrical fashion); (ii) power distributions; and (iii) overlapping durations.

In frequency-domain analysis, Welch's overlapped segment averaging estimator [39], implemented using the *pwelch* function in Matlab with a Hamming window, is performed to estimate the one-sided power spectral density (PSD). The window size, overlapping samples between adjoining sections, and number of discrete Fourier transform (DFT) points were set to 512, 256, and 512 (frequency resolution: 0.50 Hz). The values of estimated PSD are averaged over the delta (0.5–4.0 Hz), theta (4.0–8.0 Hz), alpha (8.0–13.0 Hz), and beta (13.0–30.0 Hz) bands. Moreover, the relative power in each frequency band for 14-channel voluntary eyeblink features for 20 subjects is separately compared with the relative power for involuntary eyeblink features.

In time-frequency-domain analysis, grand means of eyeblink features are used to compute spectrograms, implemented using the *spectrogram* function. The window size, overlapping samples, and number of DFT points were set at 32, 16, and 256. The log-transformed power distribution and overlapping duration are investigated from the spectrograms.

Finally, the duration of eyeblink effect in the ICs (overlapping duration of eyeblink artifacts in EEG signal), and peak amplitude value of 14-channel eyeblink features are separately computed to assess the effects of voluntary and involuntary eyeblinks on ICs contributing to EEG signals in time-domain analysis. The electrical potential caused by eyeblink will reduce its effects on EEG signals by reiteration of the positive-negative inversion, although the overall amount of discharge with eyeblink depends on the subject and the manner of eyelid/eyeball movement [14,40]. We experimentally found that the effects continue their influence for 3.0–4.0 s. In other words, each electric potential caused by an eyeblink crosses the zero points several times after passing the first positive peak; then, the potential ceases to exist. Therefore, several zero-crossing points and potential peaks are analyzed for the characterization of eyeblinks. The number will be determined in the time-frequency-domain analysis.

3. Results and discussion

In the Exp. 2, all but two subjects accomplished the criterion (90% of correct answers). The instruction got each subject to

Table 1

The number of epochs for voluntary and involuntary eyeblinks selected from each subject by visual inspection for the following analysis.

	Voluntary	Involuntary		Voluntary	Involuntary		Voluntary	Involuntary
Sub. 01	40	22	Sub. 08	11	8	Sub. 15	35	33
Sub. 02	24	20	Sub. 09	32	15	Sub. 16	30	29
Sub. 03	35	40	Sub. 10	25	18	Sub. 17	24	15
Sub. 04	13	6	Sub. 11	13	11	Sub. 18	11	11
Sub. 05	25	18	Sub. 12	13	13	Sub. 19	18	11
Sub. 06	37	40	Sub. 13	26	23	Sub. 20	17	28
Sub. 07	17	13	Sub. 14	21	20	Total	467	394

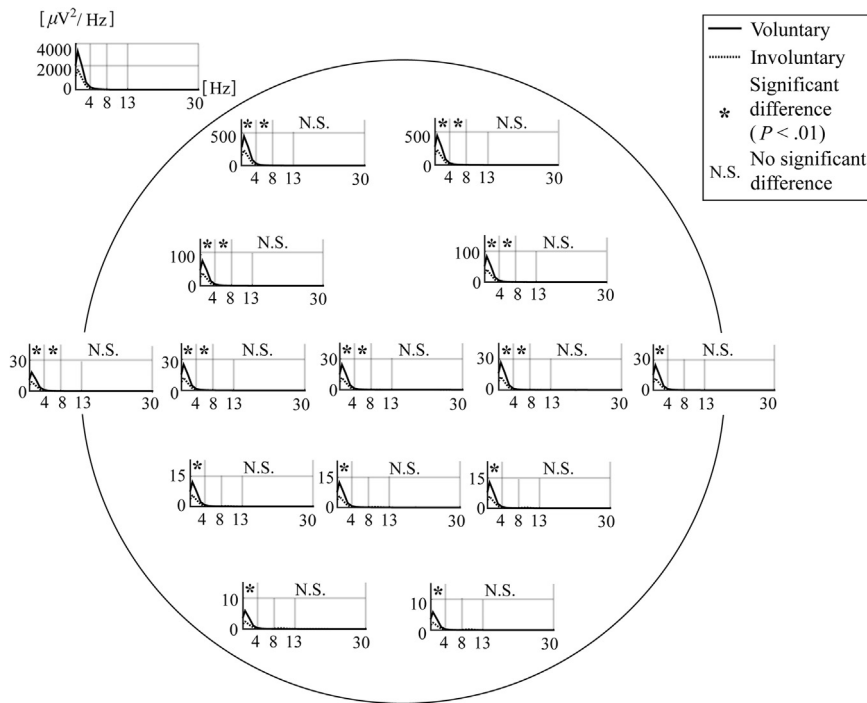


Fig. 5. Grand means of estimated PSDs at a vertical EOG (VEOG) and 14 EEG channels evaluated for voluntary (black solid line) and involuntary (black dashed line) eyeblink features; significant results at the 1% significance level are presented for the 2 blink types in each frequency band.

wholeheartedly tackle the experiments; therefore, all data were used in the analysis.

3.1. Frequency-domain analysis

Fig. 5 depicts the grand means of the estimated PSDs for 14-channel eyeblink features in EEG signals and the recorded vertical EOG (VEOG) signals, used to evaluate the differences among eyeblink features occurring under voluntary or involuntary control. The statistically significant results for two blink types are depicted together with the grand means in Fig. 5 (the bolded asterisk and N.S. indicate a significant difference and no significant difference, respectively, between voluntary and involuntary eyeblink features in the frequency band). The significance level was decided to be 1%; the results were computed for each frequency band and each EEG channel.

For eyeblinks, all of the EEG channels have a power whose frequency range and peak are less than 8 Hz and less than 4 Hz, respectively, for all eyeblink types. The power decreased with increasing distance from the eyes and the propagation of activity was proceeded along the anterior-posterior axis in a symmetrical fashion. These results support the existing literature: (i) the distorting effects of eyeblink artifacts on the EEG are within the delta

and theta bands [5,10,41]; (ii) the electric potentials (dipole projections) caused by eyeblinks decrease with increasing distance between measurement points and eyes [9,18,42]; and (iii) the propagation effects across the scalp present in a bilaterally symmetrical fashion [5,6].

In the delta band, eyeblink features extracted from all channels presented significant differences between voluntary and involuntary data. In the theta band, the eyeblink features extracted from all channels, excluding the right anterior temporal and occipital regions (T4, P3, Pz, P4, O1, and O2), presented significant differences. In contrast to these bands, there was no significant difference in the alpha and beta bands in any channels. In the real-world environment, whether an eyeblink is voluntary or involuntary is unknown. These results indicate that if an eyeblink artifact removal system had been constructed from a training dataset that contained only voluntary or involuntary eyeblink data, intrinsic EEG data might not be extricable from the recorded EEG data contaminated by eyeblink artifacts when applying the system, because there is a significant difference between voluntary and involuntary eyeblink data in the delta and theta bands.

Relative power in each frequency band and at each scalp position for voluntary and involuntary eyeblink features for 20 subjects is listed in Table 2. Eyeblink features were largely

Table 2

Averaged relative power of EEG signals measured from 14 scalp positions during voluntary and involuntary eyeblinking across 20 subjects.

Delta (0.5–4.0 Hz)		Theta (4.0–8.0 Hz)		Alpha (8.0–13.0 Hz)		Beta (13.0–30.0 Hz)		
Voluntary	Involuntary	Voluntary	Involuntary	Voluntary	Involuntary	Voluntary	Involuntary	
Fp1	0.94 ± 0.057	0.93 ± 0.053	0.03 ± 0.026	0.03 ± 0.022	0.01 ± 0.013	0.01 ± 0.018	0.02 ± 0.023	0.02 ± 0.023
Fp2	0.94 ± 0.057	0.93 ± 0.054	0.03 ± 0.026	0.03 ± 0.022	0.01 ± 0.013	0.01 ± 0.018	0.02 ± 0.023	0.02 ± 0.024
F3	0.94 ± 0.057	0.93 ± 0.053	0.03 ± 0.026	0.03 ± 0.022	0.01 ± 0.013	0.02 ± 0.017	0.02 ± 0.023	0.02 ± 0.023
F4	0.94 ± 0.057	0.93 ± 0.061	0.03 ± 0.026	0.03 ± 0.023	0.01 ± 0.014	0.02 ± 0.024	0.02 ± 0.023	0.02 ± 0.028
T3	0.94 ± 0.058	0.93 ± 0.066	0.03 ± 0.026	0.03 ± 0.024	0.01 ± 0.015	0.02 ± 0.032	0.02 ± 0.024	0.02 ± 0.025
C3	0.94 ± 0.061	0.93 ± 0.067	0.03 ± 0.032	0.03 ± 0.022	0.01 ± 0.015	0.02 ± 0.039	0.02 ± 0.023	0.02 ± 0.023
Cz	0.94 ± 0.058	0.92 ± 0.073	0.03 ± 0.026	0.03 ± 0.024	0.01 ± 0.016	0.02 ± 0.042	0.02 ± 0.023	0.02 ± 0.028
C4	0.94 ± 0.060	0.92 ± 0.090	0.03 ± 0.026	0.04 ± 0.026	0.01 ± 0.020	0.02 ± 0.055	0.02 ± 0.024	0.02 ± 0.034
T4	0.94 ± 0.060	0.91 ± 0.097	0.03 ± 0.026	0.04 ± 0.032	0.01 ± 0.019	0.02 ± 0.047	0.02 ± 0.024	0.03 ± 0.044
P3	0.94 ± 0.062	0.92 ± 0.101	0.03 ± 0.028	0.03 ± 0.024	0.01 ± 0.020	0.03 ± 0.074	0.02 ± 0.024	0.02 ± 0.026
Pz	0.93 ± 0.063	0.91 ± 0.101	0.03 ± 0.027	0.04 ± 0.027	0.01 ± 0.022	0.03 ± 0.079	0.02 ± 0.025	0.02 ± 0.032
P4	0.93 ± 0.067	0.91 ± 0.118	0.03 ± 0.026	0.04 ± 0.028	0.01 ± 0.028	0.03 ± 0.083	0.02 ± 0.025	0.03 ± 0.037
O1	0.93 ± 0.069	0.90 ± 0.137	0.03 ± 0.027	0.04 ± 0.028	0.02 ± 0.026	0.03 ± 0.092	0.02 ± 0.027	0.03 ± 0.046
O2	0.93 ± 0.063	0.91 ± 0.128	0.03 ± 0.026	0.04 ± 0.032	0.01 ± 0.020	0.03 ± 0.086	0.02 ± 0.025	0.03 ± 0.045

composed of frequency components in the delta band (over 0.90). In both types, the eyeblink artifact propagated along the spherical layer of the head, from anterior to posterior, with almost the same frequency composition. When we consider the electrodynamic models for the ocular dipole field on the scalp in spherical coordinates, the potentials generated by both eyes can be described as the scalar product of the dipole moment, where the vector depends on that placement of electrodes [9,43,44].

According to the model, decaying power should occur for an electrode located on the occipital region, because the dipole projection for the moment is lower than that of an electrode placed near the eyes. However, no channel avoids the effects of eyeblink as long as the scalp has some conductivity (zero conductivity is difficult to realize), even if the target signal derived from a source located in the occipital region. Therefore, removing the ocular potentials from all recorded EEG channels is necessary, irrespective of the installation site. *Inter alia*, research on the method of visual stimulus in the EEG signal (such as steady-state visual evoked potential-based research) often selects only the occipital region for EEG measurement positions [45]. Prudent consideration is needed to avoid eyeblink artifact contamination when the stimulus frequency used in the research is low.

3.2. Time-frequency-domain analysis

Fig. 6 shows the grand means of spectrograms of the 15 channels to investigate the overlapping duration and frequency component of eyeblink artifacts. Both eyeblink effects spread over all channels and exert a strong influence on the frontal scalp positions from Fp1 to F4. Although a similar trend of inversion is apparent in both eyeblink types, the high discharged electrical quantity of voluntary eyeblink made the eyeblink effect in EEG signals have a longer duration than that of involuntary eyeblink. As shown in the previous section, we could observe the effects only in the delta and theta bands; however, in actuality, the eyeblink effect distorts the EEG signals up to the alpha band immediately after a blink. The literature suggests that the ocular activity might not be restricted to the lower frequency region [6,46]; the results of this paper confirm this.

Both eyeblink effects decay rapidly after a blink and pass the zero-amplitude point. Then, the power rises again to a maximum value. By repeating this inversion several times, the power of the entire frequency band ceases to derive from EEG signals. For Fig. 6, two or three repetitions represented in the occipital region and other regions represent four peaks in the spectrogram. In particular, the frontal region was polluted for periods longer than other

region. The duration of the eyeblink effect in all channels is from 2 to 4 s, it was proven that our intuitive assumption is, in essence, correct. Moreover, the low frequency power remained until the end of effect, which means that the power of the low frequency band is very large compared to the power of the eyeblink effect as a whole (see Table 2).

In many studies proposing eyeblink artifact denoising techniques, 1-s epochs of EOG data including the eyeblink section are mixed with recorded EEG data to create simulated datasets for performance verification [47], or raw EEG data, which shows the effects of intentionally short and constant eyeblink intervals, is prepared for testing data [48]. Preparing simulated datasets is needed for performance verification because utilizing raw EEG data contaminated with eyeblink artifacts has the drawback that the true EEG signal is unknown [49]. However, each eyeblink artifact maintains its effect for 2 s in the EEG signals. Therefore, if researchers use epochs of EOG data including the eyeblink section for making simulated datasets or raw EEG data, which shows the effects of constant eyeblink intervals, they should use epochs of EOG data or sets with the eyeblink intervals that are 4 s or longer (if the target position is the occipital region, the lengths should be over 2 s). Otherwise, researchers will produce datasets that are similar, but not realistic.

3.3. Time-domain analysis

Fig. 7 shows the grand means and standard deviations of eyeblink features separated into 8 sampling bins, the grand means of eyeblink features and markers indicating potential peaks and zero-crossing points, plots of zero-crossing points, and a red line indicating the first positive peak of an eyeblink feature. For visualization, we used epochs at the Fp1 electrode that is placed on the prefrontal region and is sensitive to eyeblink effects. Voluntary eyeblinks had higher potentials and larger descriptions than involuntary eyeblinks [Fig. 7(A)]; therefore, the datasets of voluntary eyeblink features included large differences among individuals. On the other hand, the difference of zero-crossing time between voluntary and involuntary was not significantly different [Fig. 7(B)]. However, by sorting the plots based on the first zero-crossing point, the plots revealed an interesting eyeblink characteristic: the orchestrated crossing time is extended over a period of 500 ms after passing the third zero-amplitude point [Fig. 7(C)].

Because we could not distinguish the differences in zero-crossing time, the potential peak and zero-crossing point in each channel were compared and tabulated in Tables 3 and 4. Four

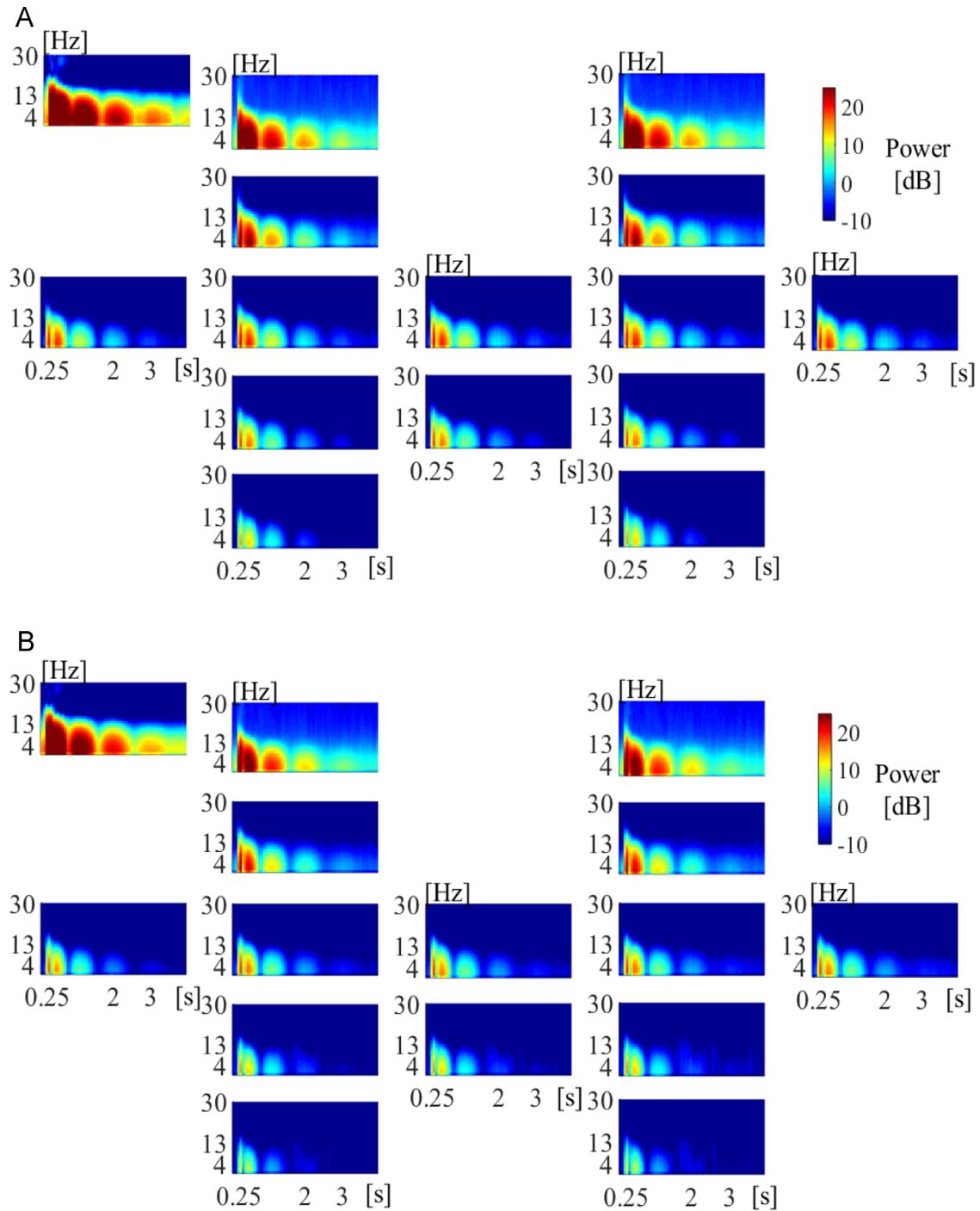


Fig. 6. (A) Grand means of spectrograms for VEOG and EEG channels for voluntary eyeblink features. (B) Grand means of spectrograms for VEOG and EEG channels for involuntary eyeblink features.

potential peaks and crossing points were analyzed in each channel; however, only three peaks and points were analyzed in the occipital region, since the effects in the regions had already ceased after passing the fourth zero-amplitude point. All potential peaks and first and second zero-crossing points in all channels were significant at the 1% significance level when compared between voluntary and involuntary. All peaks and points were at least 3 μ V for both eyeblink types. Moreover, voluntary eyeblink features had rapidly zero-crossing times, despite their high potentials.

Dry spots on the precorneal tear layer emerge 15–30 s after an eyeblink [50]; therefore, humans need a recurring cycle of

eyeblinks to maintain the ocular moisture [the normal adult eyeblink rate is roughly twenty eyeblinks/min [51]]. The upper/lower eyelid starts to move to the lower/upper eyelid with a high acceleration and reaches a peak velocity of up to 280 mm/s within 70 ms [52]. The eyelid movement is completed (zero velocity) after 100–150 ms; the reverse operation is accomplished more leisurely; it lasts roughly 300 ms. During each eyeblink, the levator palpebrae superioris muscle contracts, with a minor contribution from Müller's muscle and the orbicularis oculi muscle [53]. Spontaneous or induced eyeblink causes the eyeball to act like an electric dipole, with corneal positivity and retinal negativity [54],

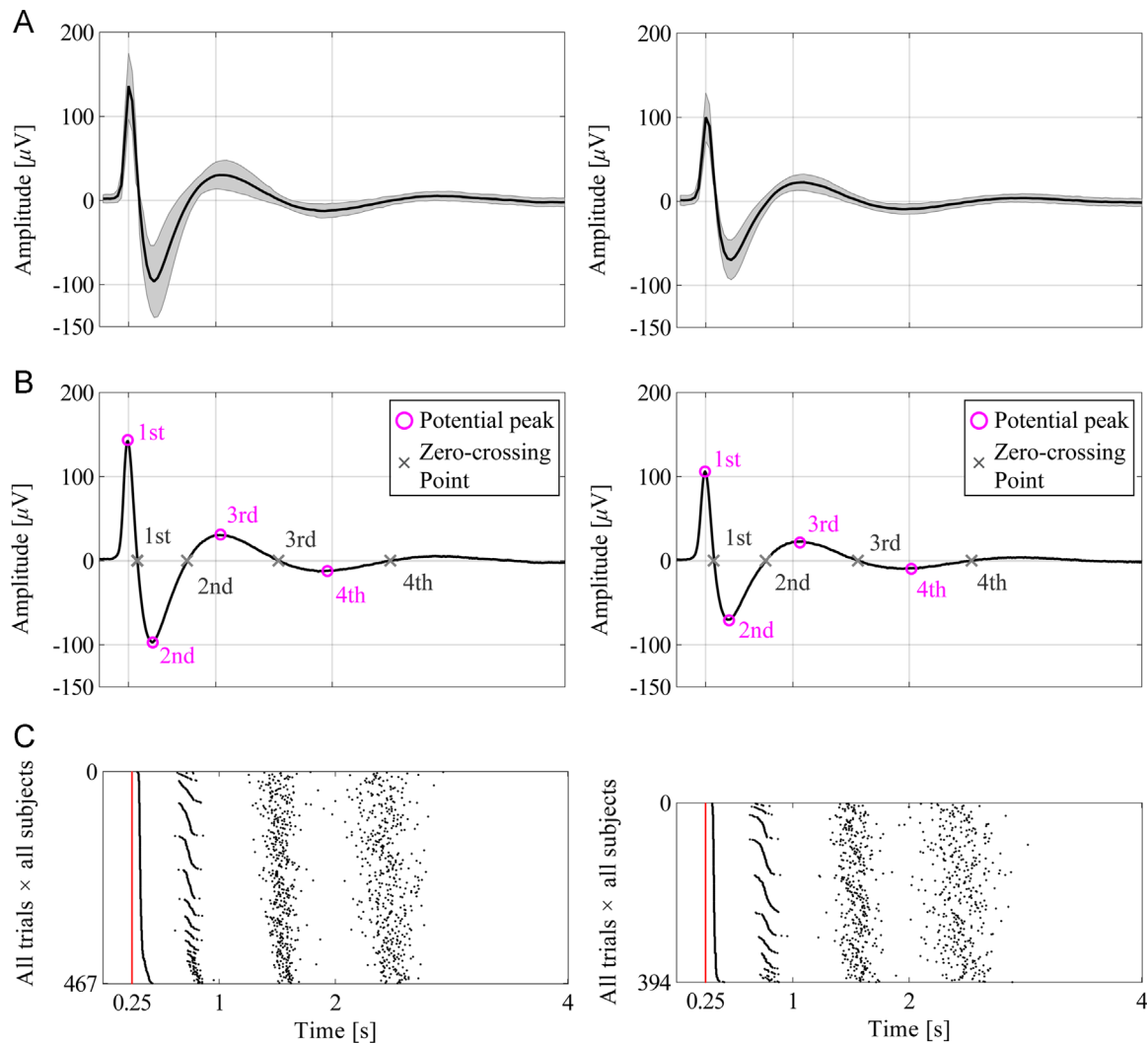


Fig. 7. Comparison between voluntary (left column) and involuntary (right column) eyeblink features in the time domain. Eyeblink features obtained at the Fp1 position were selected for visualization because the prefrontal area is nearest to the eyes and is most affected by eyeblink. (A) Grand means and SDs of eyeblink features separated into 8 sampling bins. (B) Grand means of eyeblink features and markers indicating potential peaks (pink circles) and zero-crossing points (gray x-marks). The markers of each feature are presented in Tables 3 and 4 to allow statistical comparison of the two eyeblink types. (C) Plots of zero-crossing points and a red line indicating the first positive peak of an eyeblink feature. The data is sorted based on the first zero-crossing points. (For interpretation of the references to color in this figure legend, the reader is referred to the web version of this article.)

Table 3

Averaged absolute value of amplitude (μV) and latency (s) of voluntary eyeblink data at the first four potential peaks and zero-crossing points from the stimulus onset, respectively.

	First		Second		Third		Fourth	
	Potential peak [μV]	Zero-crossing [s]						
Fp1	146.45 ± 40.2	0.33 ± 0.021	109.34 ± 49.6	0.75 ± 0.042	39.89 ± 19.2	1.53 ± 0.083	23.34 ± 9.4	2.44 ± 0.144
Fp2	145.89 ± 40.0	0.33 ± 0.021	109.11 ± 48.7	0.75 ± 0.043	39.73 ± 18.6	1.53 ± 0.086	23.30 ± 9.3	2.42 ± 0.160
F3	61.94 ± 17.0	0.33 ± 0.021	46.39 ± 21.2	0.75 ± 0.043	16.97 ± 8.4	1.53 ± 0.087	9.95 ± 4.2	2.42 ± 0.165
F4	61.12 ± 17.9	0.33 ± 0.022	45.77 ± 21.4	0.75 ± 0.043	16.72 ± 8.6	1.52 ± 0.090	9.86 ± 4.4	2.41 ± 0.164
T3	29.91 ± 9.1	0.33 ± 0.021	22.61 ± 11.9	0.75 ± 0.043	8.33 ± 4.7	1.52 ± 0.094	4.94 ± 2.4	2.41 ± 0.161
C3	34.08 ± 10.1	0.33 ± 0.021	25.37 ± 11.7	0.75 ± 0.045	9.36 ± 4.8	1.52 ± 0.092	5.50 ± 2.4	2.40 ± 0.170
Cz	32.58 ± 10.7	0.33 ± 0.021	24.20 ± 11.6	0.75 ± 0.043	8.92 ± 4.9	1.52 ± 0.089	5.28 ± 2.5	2.41 ± 0.165
C4	33.43 ± 11.0	0.33 ± 0.022	24.95 ± 12.4	0.75 ± 0.043	9.19 ± 5.2	1.52 ± 0.090	5.44 ± 2.7	2.41 ± 0.169
T4	31.04 ± 11.6	0.33 ± 0.022	23.23 ± 13.0	0.75 ± 0.043	8.55 ± 5.4	1.52 ± 0.096	5.09 ± 2.9	2.40 ± 0.170
P3	23.02 ± 7.7	0.33 ± 0.021	17.09 ± 8.3	0.75 ± 0.043	6.31 ± 3.5	1.52 ± 0.087	—	—
Pz	22.73 ± 8.3	0.33 ± 0.021	16.83 ± 8.5	0.75 ± 0.044	6.24 ± 3.6	1.52 ± 0.101	—	—
P4	22.81 ± 8.5	0.33 ± 0.021	16.95 ± 9.0	0.75 ± 0.043	6.27 ± 3.8	1.52 ± 0.099	—	—
O1	15.11 ± 6.6	0.33 ± 0.021	11.24 ± 6.7	0.75 ± 0.043	4.19 ± 2.8	1.52 ± 0.105	—	—
O2	14.61 ± 7.2	0.33 ± 0.021	10.88 ± 7.2	0.75 ± 0.043	4.02 ± 3.1	1.52 ± 0.095	—	—

Table 4

Averaged absolute value of amplitude (μ V) and latency (s) of involuntary eyeblink data at the first four potential peaks and zero-crossing points from the stimulus onset, respectively.

First	Second		Third		Fourth			
	Potential peak [μ V]	Zero- crossing [s]	Potential peak [μ V]	Zero- crossing [s]	Potential peak [μ V]	Zero- crossing [s]	Potential peak [μ V]	Zero- crossing [s]
Fp1	109.04 \pm 30.1	0.33 \pm 0.011	77.13 \pm 24.9	0.77 \pm 0.047	31.88 \pm 9.7	1.54 \pm 0.096	20.18 \pm 6.3	2.44 \pm 0.166
Fp2	109.04 \pm 28.4	0.33 \pm 0.011	77.35 \pm 24.0	0.77 \pm 0.047	32.08 \pm 9.4	1.54 \pm 0.101	20.30 \pm 6.3	2.42 \pm 0.176
F3	45.69 \pm 12.1	0.33 \pm 0.011	32.48 \pm 10.8	0.77 \pm 0.047	13.47 \pm 4.3	1.55 \pm 0.099	8.58 \pm 2.9	2.42 \pm 0.179
F4	45.46 \pm 11.6	0.33 \pm 0.011	32.43 \pm 10.6	0.77 \pm 0.048	13.60 \pm 4.3	1.54 \pm 0.101	8.74 \pm 3.0	2.42 \pm 0.184
T3	21.34 \pm 5.9	0.33 \pm 0.011	15.20 \pm 5.3	0.77 \pm 0.047	6.31 \pm 2.1	1.54 \pm 0.103	4.09 \pm 1.6	2.41 \pm 0.191
C3	24.85 \pm 6.8	0.33 \pm 0.011	17.67 \pm 6.0	0.77 \pm 0.047	7.37 \pm 2.5	1.54 \pm 0.100	4.79 \pm 1.9	2.41 \pm 0.187
Cz	23.98 \pm 6.6	0.33 \pm 0.011	17.13 \pm 5.8	0.77 \pm 0.048	7.24 \pm 2.5	1.54 \pm 0.106	4.76 \pm 2.0	2.42 \pm 0.186
C4	24.90 \pm 6.7	0.33 \pm 0.011	17.86 \pm 6.1	0.77 \pm 0.051	7.61 \pm 2.6	1.54 \pm 0.101	5.06 \pm 2.4	2.41 \pm 0.190
T4	23.51 \pm 6.6	0.33 \pm 0.012	16.94 \pm 6.0	0.77 \pm 0.052	7.32 \pm 2.7	1.54 \pm 0.108	4.89 \pm 2.5	2.41 \pm 0.193
P3	16.48 \pm 4.9	0.33 \pm 0.013	11.81 \pm 4.3	0.77 \pm 0.049	5.04 \pm 2.2	1.54 \pm 0.106	—	—
Pz	16.33 \pm 5.0	0.33 \pm 0.011	11.71 \pm 4.4	0.77 \pm 0.050	5.06 \pm 2.4	1.53 \pm 0.119	—	—
P4	16.69 \pm 5.1	0.33 \pm 0.011	12.05 \pm 4.6	0.76 \pm 0.053	5.28 \pm 2.7	1.52 \pm 0.129	—	—
O1	10.48 \pm 4.0	0.33 \pm 0.013	7.61 \pm 3.5	0.77 \pm 0.053	3.46 \pm 2.4	1.52 \pm 0.124	—	—
O2	10.48 \pm 4.0	0.33 \pm 0.012	7.61 \pm 3.5	0.76 \pm 0.054	3.39 \pm 2.1	1.52 \pm 0.133	—	—

slightly moving up/down and inward [55]. Therefore, the above-mentioned factors produce electrical potentials after an eyeblink, and these potentials are mixed with the respective potentials on the scalp in the electrooculographic (EOG) signal, which can be recorded using two electrodes placed at the superior and inferior orbital rims of the eyes.

We described how eyelid and eyeball movements influence the electrical potential in complex ways in preceding paragraph. The first positive potential is caused by combining up/down and inward eyeball movements (dipole rotation changing) and the sliding eyelid on a positively charged cornea [9,14] with extraocular muscle co-contraction. In contrast to the stated blink motions, the first negative potential is caused by combining the down/up and outward eyeball movements and inverse eyelid movement. The third and fourth potential peaks (second positive and negative potentials) were caused not only by the eyeblink potential occurring at right and left eyes respectively but also each simultaneous potential and three-dimensional diffusion, similar to circular wave patterns in the brain. In our opinion, the diffused potentials would pile up at a specific point within the cranium and the magnified potential would reach each electrode. However, it is known that EEG signals generated from mammal brains have high-spatiotemporal complexity and that the cortical connectivity is very highly weighted toward short ($< 500 \mu$ V) connections, which means that neuronal activities spread through a contiguous cortical region with a high attenuation penalty, based on the distance from sources [56,57]. The ICA algorithm successfully accomplishes source separation of EEG signals because of these dynamics [22]. The attenuation penalty with increasing distance may affect the genuineness of our supposition; nevertheless, the propagation path of the EOG potential does not determine whether the EOG penalty coefficient is identical to that of the EEG. Therefore, this is simply our opinion.

4. Conclusions

In this paper, the effect of voluntary and involuntary eyeblinks on ICs contributing to EEG signals was characterized for creating templates of eyeblink artifact rejection from recorded EEG signals with small number of electrodes. Fourteen EEG signals and one vertical EOG signal were recorded for twenty healthy subjects during two different experiments, which prompted subjects to blink voluntarily and involuntarily. Wavelet-enhanced ICA with two markers (mMSE and kurtosis) was employed as a source-

separation and feature-extraction scheme. The extracted eyeblink features were separated into epochs and analyzed in the frequency, time-frequency, and time domains.

The extracted eyeblink features confirmed three characteristics reported in the literature: (i) the distorting effects of eyeblink artifacts on the EEG are within the delta and theta bands; (ii) electric potentials (dipole projections) caused by eyeblinks decrease with increasing distance between measurement points and eyes; and (iii) the propagation effects across the scalp present in a bilaterally symmetrical fashion. Furthermore, additional characteristics were found: (i) eyeblink features obtained from all channels presented significant differences between voluntary and involuntary; (ii) eyeblink effects continue to have an influence on EEG signals for 3.0–4.0 s (in the occipital region, 2.0 s); and (iii) these effects cease to exist after the zero-crossing point four (in the occipital region: two) times, for both eyeblink types.

Eyeblink artifactual contamination, which inevitably occurs with EEG applications, should be rejected from recorded EEG signals to allow precise diagnosis and system construction. The differences among the effects of voluntary and involuntary eyeblink in EEG signals were shown in this paper. The datasets used in this study is freely available (<http://u4ag2kanosr1.blogspot.jp/>). These results and dataset are helpful for making templates of eyeblink artifact rejection from recorded EEG signals with small number of electrodes. Finally, we hope the heuristic development of more robust and more common references and training data based on the representative attributes for small number of channels in EEG analysis and encourage the practical use of EEG applications in daily life.

Author contributions

Conceived and designed the experiments: SK. Performed the experiments: SK. Analyzed the data: SK. Wrote the paper: SK, MN, and YM.

Acknowledgments

This work was supported by JSPS KAKENHI Grant number 15H02235.

References

- [1] M. Koukkou, D. Lehmann, J. Wackermann, I. Dvorak, B. Henggeler, Dimensional complexity of EEG brain mechanisms in untreated schizophrenia, *Biol. Psychiatry* 33 (6) (1993) 397–407.
- [2] P.G. Rossi, A. Parmegiani, V. Bach, M. Santucci, P. Visconti, EEG features and epilepsy in patients with autism, *Brain Dev.* 17 (3) (1995) 169–174.
- [3] L.A. Farwell, E. Donchin, Talking off the top of your head: toward a mental prosthesis utilizing event-related brain potentials, *Electroencephalogr. Clin. Neurophysiol.* 70 (6) (1988) 510–523.
- [4] J.R. Wolpaw, N. Birbaumer, D.J. McFarland, G. Pfurtscheller, T.M. Vaughan, Brain-computer interfaces for communication and control, *Clin. Neurophysiol.* 113 (6) (2002) 767–791.
- [5] T. Gasser, L. Sroka, J. Möcks, The transfer of EOG activity into the EEG for eyes open and closed, *Electroencephalogr. Clin. Neurophysiol.* 61 (2) (1985) 181–193.
- [6] D. Hagemann, E. Naumann, The effects of ocular artifacts on (lateralized) broadband power in the EEG, *Clin. Neurophysiol.* 112 (2) (2001) 215–231.
- [7] W.G. Iacono, D.T. Lykken, Two-year retest stability of eye tracking performance and a comparison of electro-oculographic and infrared recording techniques: evidence of EEG in the electro-oculogram, *Psychophysiology* 18 (1) (1981) 49–55.
- [8] O.G. Lins, T.W. Picton, P. Berg, M. Scherg, Ocular artifacts in EEG and event-related potentials I: scalp topography, *Brain Topogr.* 6 (1) (1993) 51–63.
- [9] T. Elbert, W. Lutzenberger, B. Rockstroh, N. Birbaumer, Removal of ocular artifacts from the EEG—a biophysical approach to the EOG, *Electroencephalogr. Clin. Neurophysiol.* 60 (5) (1985) 455–463.
- [10] G. Gratton, Dealing with artifacts: the EOG contamination of the event-related brain potential, *Behav. Res. Methods Instrum. Comput.* 30 (1) (1998) 44–53.
- [11] R. Verleger, The instruction to refrain from blinking affects auditory P3 and N1 amplitudes, *Electroencephalogr. Clin. Neurophysiol.* 78 (3) (1991) 240–251.
- [12] J.C. Woestenburg, M.N. Verbaten, J.L. Slangen, The removal of the eye-movement artifact from the EEG by regression analysis in the frequency domain, *Biol. Psychol.* 16 (1) (1983) 127–147.
- [13] G. Gratton, M.G. Coles, E. Donchin, A new method for off-line removal of ocular artifact, *Electroencephalogr. Clin. Neurophysiol.* 55 (4) (1983) 468–484.
- [14] F. Matsuo, J.F. Peters, E.L. Reilly, Electrical phenomena associated with movements of the eyelid, *Electroencephalogr. Clin. Neurophysiol.* 38 (5) (1975) 507–511.
- [15] R.E. Records, *Physiology of the Human Eye and Visual System*, Harper and Row, Hagerstown, 1979.
- [16] S. Hoffmann, M. Falkenstein, The correction of eye blink artefacts in the EEG: a comparison of two prominent methods, *PLoS One* 3 (8) (2008) e3004.
- [17] T.P. Jung, S. Makeig, C. Humphries, T.W. Lee, M.J. McKeown, V. Irugui, T.J. Sejnowski, Removing electroencephalographic artifacts by blind source separation, *Psychophysiology* 37 (02) (2000) 163–178.
- [18] T. Gasser, P. Ziegler, W.F. Gattaz, The deleterious effect of ocular artefacts on the quantitative EEG, and a remedy, *Eur. Arch. Psychiatry. Clin. Neurosci.* 241 (6) (1992) 352–356.
- [19] A.J. Bell, T.J. Sejnowski, An information-maximization approach to blind separation and blind deconvolution, *Neural Comput.* 7 (6) (1995) 1129–1159.
- [20] P. Comon, Independent component analysis, a new concept, *Signal Process.* 36 (3) (1994) 287–314.
- [21] S. Makeig, A.J. Bell, T.P. Jung, T.J. Sejnowski, Independent component analysis of electroencephalographic data, *Adv. Neural Inf. Process. Syst.* 8 (1996) 145–151.
- [22] J. Onton, S. Makeig, Information-based modeling of event-related brain dynamics, *Prog. Brain Res.* 159 (2006) 99–120.
- [23] H. Serby, E. Yom-Tov, G.F. Inbar, An improved P300-based brain-computer interface, *IEEE Trans. Neural Syst. Rehabil. Eng.* 13 (1) (2005) 89–98.
- [24] S. Romero, M.A. Mañanas, M.J. Barbanjo, A comparative study of automatic techniques for ocular artifact reduction in spontaneous EEG signals based on clinical target variables: a simulation case, *Comput. Biol. Med.* 38 (3) (2008) 348–360.
- [25] M.E. Davies, C.J. James, Source separation using single channel ICA, *Signal Process.* 87 (8) (2007) 1819–1832.
- [26] B. Mijović, M. De Vos, I. Gligorijević, J. Taelman, S. Van Huffel, Source separation from single-channel recordings by combining empirical-mode decomposition and independent component analysis, *IEEE Trans. Biomed. Eng.* 57 (9) (2010) 2188–2196.
- [27] H. Peng, B. Hu, Q. Shi, M. Ratcliffe, Q. Zhao, Y. Qi, G. Gao, Removal of ocular artifacts in EEG—an improved approach combining DWT and ANC for portable applications, *IEEE J. Biomed. Health Inform.* 17 (3) (2013) 600–607.
- [28] Y. Li, Z. Ma, W. Lu, Y. Li, Automatic removal of the eye blink artifact from EEG using an ICA-based template matching approach, *Physiol. Meas.* 27 (4) (2006) 425–436.
- [29] N.P. Castellanos, V.A. Makarov, Recovering EEG brain signals: artifact suppression with wavelet enhanced independent component analysis, *J. Neurosci. Methods* 158 (2) (2006) 300–312.
- [30] D.H. Brainard, The psychophysics toolbox, *Spat. Vis.* 10 (1997) 433–436.
- [31] A. Yagi, Visual signal detection and lambda responses, *Electroencephalogr. Clin. Neurophysiol.* 52 (6) (1981) 604–610.
- [32] D.I. McCloskey, Corollary discharges: motor commands and perception, *Compr. Physiol.* (1981).
- [33] A. Delorme, S. Makeig, EEGLAB: an open source toolbox for analysis of single-trial EEG dynamics including independent component analysis, *J. Neurosci. Methods* 134 (1) (2004) 9–21.
- [34] T.P. Jung, S. Makeig, M. Westerfield, J. Townsend, E. Courchesne, T.J. Sejnowski, Removal of eye activity artifacts from visual event-related potentials in normal and clinical subjects, *Clin. Neurophysiol.* 111 (10) (2000) 1745–1758.
- [35] G.L. Wallstrom, R.E. Kass, A. Miller, J.F. Cohn, N.A. Fox, Automatic correction of ocular artifacts in the EEG: a comparison of regression-based and component-based methods, *Int. J. Psychophysiol.* 53 (2) (2004) 105–119.
- [36] R. Mahajan, B. Morshed, Unsupervised eye blink artifact denoising of EEG data with modified multiscale sample entropy, kurtosis and wavelet-ICA, *IEEE J. Biomed. Health Inf.* 19 (1) (2015) 158–165.
- [37] H.B. Xie, W.X. He, H. Liu, Measuring time series regularity using nonlinear similarity-based sample entropy, *Phys. Lett. A* 372 (48) (2008) 7140–7146.
- [38] A. Delorme, T. Sejnowski, S. Makeig, Enhanced detection of artifacts in EEG data using higher-order statistics and independent component analysis, *Neuroimage* 34 (4) (2007) 1443–1449.
- [39] P.D. Welch, The use of fast Fourier transform for the estimation of power spectra: a method based on time averaging over short, modified periodograms, *IEEE Trans. Audio Electroacoust.* 15 (2) (1967) 70–73.
- [40] J.C. Corby, B.S. Kopell, Differential contributions of blinks and vertical eye movements as artifacts in EEG recording, *Psychophysiology* 9 (6) (1972) 640–644.
- [41] J. Möcks, T. Gasser, How to select epochs of the EEG at rest for quantitative analysis, *Electroencephalogr. Clin. Neurophysiol.* 58 (1) (1984) 89–92.
- [42] P.L. Nunez, R. Sriinivasan, *Electric Fields of the Brain: The Neurophysics of EEG*, Oxford University Press, New York, NY, 2006.
- [43] P. Berg, M. Scherg, Dipole models of eye movements and blinks, *Electroencephalogr. Clin. Neurophysiol.* 79 (1) (1991) 36–44.
- [44] B.N. Cuffin, D. Cohen, Comparison of the magnetoencephalogram and electroencephalogram, *Electroencephalogr. Clin. Neurophysiol.* 47 (2) (1979) 132–146.
- [45] D. Zhu, J. Bieger, G.G. Molina, R.M. Aarts, A survey of stimulation methods used in SSVEP-based BCIs, *Comput. Intell. Neurosci.* 2010 (1) (2010) 1–12.
- [46] J. Ma, S. Bayram, P. Tao, V. Svetniki, High-throughput ocular artifact reduction in multichannel electroencephalography (EEG) using component subspace projection, *J. Neurosci. Methods* 196 (1) (2011) 131–140.
- [47] M.L. Shoker, S. Sanei, W. Wang, J.A. Chambers, Removal of eye blinking artifact from the electro-encephalogram, incorporating a new constrained blind source separation algorithm, *Med. Biol. Eng. Comput.* 43 (2) (2005) 290–295.
- [48] V. Krishnaveni, S. Jayaraman, A. Gunasekaran, K. Ramadoss, Automatic removal of ocular artifacts using JADE algorithm and neural network, *Int. J. Intell. Syst. Technol.* 1 (4) (2006) 322–333.
- [49] Q. Zhao, B. Hu, Y. Shi, Y. Li, P. Moore, M. Sun, H. Peng, Automatic identification and removal of ocular artifacts in EEG—improved adaptive predictor filtering for portable applications, *IEEE Trans. NanoBiosci.* 13 (2) (2014) 109–117.
- [50] M.G. Doane, Interaction of eyelids and tears in corneal wetting and the dynamics of the normal human eyeblink, *Am. J. Ophthalmol.* 89 (4) (1980) 507–516.
- [51] C.N. Karson, Spontaneous eye-blink rates and dopaminergic systems, *Brain* 106 (3) (1983) 643–653.
- [52] H. Collewijn, J. Van der Steen, R.M. Steinman, Human eye movements associated with blinks and prolonged eyelid closure, *J. Neurophysiol.* 54 (1) (1985) 11–27.
- [53] A. Ettl, S. Priglinger, J. Kramer, L. Koornneef, Functional anatomy of the levator palpebrae superioris muscle and its connective tissue system, *Br. J. Ophthalmol.* 80 (8) (1996) 702–707.
- [54] P. Berg, M. Scherg, Dipole modelling of eye activity and its application to the removal of eye artefacts from the EEG and MEG, *Clin. Phys. Physiol. Meas.* 12 (A) (1991) 49–54.
- [55] M. Iwasaki, C. Kellinghaus, A.V. Alexopoulos, R.C. Burgess, A.N. Kumar, Y.H. Han, H.O. Lüders, R.J. Leigh, Effects of eyelid closure, blinks, and eye movements on the electroencephalogram, *Clin. Neurophysiol.* 116 (4) (2005) 878–885.
- [56] A. Arieli, A. Sterkin, A. Grinvald, A. Aertsen, Dynamics of ongoing activity: explanation of the large variability in evoked cortical responses, *Science* 273 (5283) (1996) 1868–1871.
- [57] W.J. Freeman, Origin, structure, and role of background EEG activity. Part 1. Analytic amplitude, *Clin. Neurophysiol.* 115 (9) (2004) 2077–2088.



Suguru Kanoga received his M.E. degree from Keio University, Kanagawa, Japan, in 2014. He is a research fellow of Japan Society for Promotion of Science, Japan from 2015. He is currently with the School of Integrated Design Engineering, Keio University. His research interests include artifact rejection for biomedical signal processing and prosthesis control with surface EMG.



Masaki Nakanishi received his M.E degrees from Tokyo University of Agriculture and Technology, Tokyo, Japan, in 2009 and 2010, respectively, and the Ph.D. degree in engineering from Keio University, Kanagawa, Japan, in 2014. He was a research fellow of Japan Society for Promotion of Science, Japan, in 2013–2015. He is currently a postdoctoral researcher at the Swartz Center for Computational Neuroscience, University of California San Diego. His research interests include brain-computer interface and biomedical signal processing.



Yasue Mitsukura received her D.R. degree from the University of Tokushima, Tokushima, Japan, in 2001. She worked at the University of Tokushima and Okayama University as an Assistant Professor and a Lecturer, respectively. Since 2011, she has been an Associate Professor at Keio University. Her research interests are biomedical signal processing and image signal processing. She is a member of SICE, IEEJ, RISP, and IEEE.